Research Article

Ákos Kereszturi*, Ludovic Duvet, Gyula Gróf, Ákos Gyenis, Tamás Gyenis, Zsuzsanna Kapui, Bálint Kovács, and Gyula Maros

Characterization and first results of the planetary borehole-wall imager — methods to develop for in-situ exploration

https://doi.org/10.1515/astro-2019-0001
Received Mar 18, 2018; accepted Jun 11, 2018

Abstract: Prototypes of borehole-wall imager instruments were developed and tested at a desert riverbed in Morocco and at a lake's salty flat in the Atacama desert, to support the drilling activity of ExoMars rover. The onsite recorded borehole images contain information on the context that are lost during the sample acquisition. Benefits of the borehole-wall imaging is the easier maximal energy estimation of a fluvial flow, the detailed information on sedimentation and layering, especially the former existence of liquid water and its temporal changes, including paleo-flow direction estimation from grain imbrication direction. Benefits of laboratory analysis of the acquired samples are the better identification of mineral types, determination of the level of maturity of granular sediment, and identification of the smallest, wet weathered grains. Based on the lessons learned during the comparison of field and laboratory results, we demonstrate that recording the borehole-wall with optical instrument during/after drilling on Mars supports the paleo-environment reconstruction with such data that would otherwise be lost during the sample acquisition. Because of the lack of plate tectonism and the low geothermal gradient on Mars, even Ga old sediments provide observable features that are especially important for targeting Mars sample return and later crewed Mars missions.

Keywords: Mars, drilling, sample analysis

1 Introduction

The aim of this work is to compare the potential results of two different in-situ sample analysing methods for planetary bodies: the poorly tested optical scanning of borehole-wall and the more widely used optical analysis under laboratory conditions of the acquired sample. While in the first case the samples are surveyed as they are embedded in their original environment, in the second case the collected samples are analysed without their original context. (For more detailed background information on these methods please see the next subchapter.) Future Mars missions will heavily exploit in-situ work, sample return and rely on material obtained from borehole, as biologically relevant target is expected to survive at meter depth there so drilling is required to reach it. Thus, it is worth testing the possible benefits at Mars analogue sites (Groemer et al. 2014) for how such two observation types are complementary, which were already partly tested at diverse geological conditions (Losiak et al. 2013; Orgel et al. 2013b), to develop technology (Foing et al. 2011a) with focus on astrobiology related activities (Foing et al. 2011b) and also on logistics related to human work performance (Groemer et al. 2010; Orgel et al. 2013a).

During the Mars sample return and especially planned future crewed mission, the sample selection on Mars requires careful work, and the efficiency of sample targeting and selection should be supported by such local analysis that provides information on the depositional conditions and local context too. Drilling is an important method for sample acquisition on Mars as various UV (Moores and Schuerger 2012; Poch et al. 2014; Stalport et al. 2009) and particle radiation (Dartnell and Patel 2014), as well as at-

Corresponding Author: Ákos Kereszturi: Research Centre for Astronomy and Earth Sciences, Hungary;
Email: akos.kereszturi@csfk.mta.hu
Ludovic Duvet: European Space Agency, ESTEC, The Netherlands
Gyula Gróf, Tamás Gyenis, Bálint Kovács: Budapest University of Technology and Economics, Hungary
Ákos Gyenis: Kolorprint LP. Hungary
Zsuzsanna Kapui: Research Centre for Astronomy and Earth Sciences, Hungary
Gyula Maros: Mining and Geological Survey of Hungary

mospheric generated oxidants (Benner et al. 2000; Zent and McKay 1993) on the surface could destroy biosignatures (Westall et al. 2015). As old sedimentary strata might hold information on habitable conditions, on-site analysis of the borehole-wall during the drill is helpful. In this work, the related technology and the first results for such analysis is presented.

Future missions need to have subsurface access, *e.g.* drilling on Mars (Ori et al. 2000; Parro et al. 2008; Stoker et al. 2008) and the potential of data acquisition during the drill should be tested beforehand. Despite that, surveying the borehole-wall during drilling might provide ideal context to better understand the acquired samples' properties, only a small amount of effor is aimed to exploit this possibility. MaMISS instrument onboard the driller of the ExoMars 2020 rover of ESA (De Angelis et al. 2014) will scan both horizontally and vertically the borehole-wall in the near infrared but not in the optical range. In this paper, we summarize the related background knowledge from the Earth firstly, then give general characteristics of the borehole-wall imagers used in this project secondly, and finally present the results of field and laboratory sample analysis. In the Discussion section, we compare the advantages and disadvantages of the in-situ and laboratory methods. Using these experiences, we provide suggestions how the capabilities could be exploited for further missions and which of those capabilities should be developed further to reach an ideal system to identify past conditions during drilling and sampling on Mars.

1.1 Background information: drilling on Earth and Mars

In classical Earth sciences, especially in applied research in petroleum industry, as well as in the search for water and other resources, drilling based subsurface exploration is regularly used (Castagna and Bellin 2009; Cheng 1981; Daily et al. 1992; Rehfeldt et al. 1992; Wang 1992). In addition, research drills are made regularly for reconnaissance exploration. In these cases the drilled core is analysed macroscopically firstly, and then microscopically too. Used technologies for borehole analysis, however, mainly focus on geophysical characteristics like conductivity, porosity, material strength acquired during the drill (providing unique information on rock permeability, spatial density of fractures, deformation style etc.) – but optical analysis was rarely performed. The produced logs are mainly done inside water, mud or hydrocarbon filled boreholes, dry boreholes are rarely analysed – however on Mars, future missions will meet with this type of boreholes.

Possibility and expected performance of drills for Mars were analysed based on theoretical argumentations, laboratory and Earth analogues field tests (Finzi et al. 2004; McKay et al. 2007) previously. Drilling in permafrost terrain found to be possible (Zacny et al. 2013a) however several technical difficulties including the prevention from melting emerge, while thermal drill is also a possible approach (Weiss et al. 2008) there. Planetary protection issues should be considered during any drill activity (Christner et al. 2005; Juck et al. 2005) thus proper sterilization is required. Drilling in regolith was tested to improve the drill head design (Pitcher and Gao 2015), and testing were made for specific dual-reciprocating drilling (Gouache et al. 2011), tethered supported Down-Hole-Motor Drilling (Hill et al. 2003), coiled tubing drilling and mole drilling (Hoftun et al. 2013) were also evaluated. Laboratory tests demonstrated that even small gas flow under Mars relevant conditions could eject the small cuttings from the borehole (Zacny et al. 2004) by the sublimation of ice in the drilled hole. The low temperature increases the strength of the target rocks, making more energy consuming the drilling process on Mars (Zacny et al. 2009).

The drilling produced temperature increase was also analysed (Szwarc et al. 2012), and the use of single drills as well as multiple rods were demonstrated that might be successful under Mars like conditions (Magnani et al. 2004). Autonomous decisions and performance were also tested (Glass et al. 2008) what is required to realize a drill on Mars, however teleoperation from Martian orbit may be also possible in the future (Glass et al. 2012; Lee et al. 2009). Several parts of the drilling process were tested and demonstrated with successful performance, just like sample acquisition and transport (Zacny et al. 2013b) in the Antarctic Dry Valleys and in the Atacama desert (Zacny et al. 2015), at Haughton crater in arctic Canada (Glass et al. 2006), at Rio Tinto in Spain (Prieto-Ballesteros et al. 2008), and at the Gypsum Quarry at Borrego Springs, California (Zacny et al. 2013c). Under the planned Canadian Norhtern Light Mission several Mars relevant aspects will be tested of a drilling on Mars (Navarathinam et al. 2011).

During drilling the optical analysis of the borehole-wall has not been planned or tested beyond that of the Earth (except the already mentioned infrared imaging capability of MaMISS). On the Earth optical method recorded with televiewer (Philippe et al. 2007) was used in coupled to acoustic data (Williams and Johnson 2004) to identify and analyse the spatial density of fractures which could be better identified by acoustic than optical method, while optical images allowed to understand the relation between fractures and the lithology plus bedding. Optical televiewers are also used to identify borehole breakouts that point

to fractures and stress in the host rock. Beside the often analysed tectonic structures, sedimentary and diagenetic features could be also identified on borehole-wall images. Some background experiences exist from the Earth, however the method should be further developed for Mars, and this work provides some specific input for that regarding the analysis of sediments at Mars analogue terrains.

2 Material and methods

During the research work a first version of a subsurface optical detector and an advanced second version of the fully built borehole-wall imager were used. The targets were Mars analogue materials at field sites in Morocco and Chile, where the targets were not only imaged at their original context but were acquired as samples for later laboratory work in Hungary. Below, the field sites are described first followed by the used facilities.

During the **field activity** in Morocco at the Ibn Battua Center's field sites (Kapui et al. 2017) (15-21 in September, 2016) in-situ survey with the first version of the camera (Figure 1) together with sampling for subsequent laboratory analysis were applied. The samples were acquired at 30.983N, 7.153W around 2 km to west from Timedline in a desert wadi. While the fully built version of the borehole-wall imager (Figure 2) was tested in the Atacama desert at the salty lake of Laguna Verde, inside clayey sediments (11-28 February, 2018). At the field manual drilling by soil corer of soft sediments were made, the sample acquisition of the pulled out core happened firstly, while image recording of the drilled borehole was done secondly. Documentation for the nearby outcrop wall at the depth values of the acquired samples were also made subsequently.

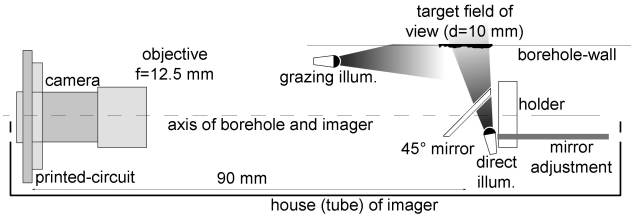

Figure 1. Schematic structure of the imager with the camera at the left that views a segment of the wall by a mirror (top right). The direct illumination provides light to the target not trough the mirror, however on this image it is visualized this way).

Besides testing the observability under different conditions, we compared the field recorded and **laboratory** recorded images in order to identify the favourable and

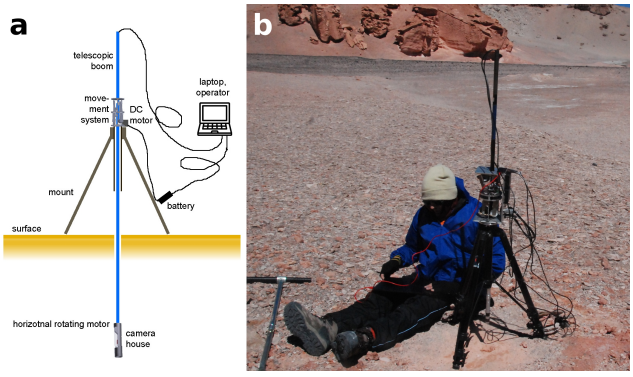

Figure 2. Generalized structure of the borehole-wall scanning system (a) and its usage in the Atacama desert at Laguna Verde (b).

unfavourable aspects of the performance, including the size distribution, shape characteristics and related observational possibilities of grains. For the laboratory analysis the field acquired samples were transported to the home institute, and as they were weakly cemented, many aggregates were fallen into pieces, thus supporting the analysis of grains separately. The laboratory conditions for image recording, were better but the same camera was used as in the field, while geometry and focusing issues were also better solved there. Two types of imaging were made in the laboratory: using the same imager like in the field and a more sophisticated microscope, by NICON Eclipse E600 POL, which has 4x, 10x, 20x and 40x magnification.

For the analysis of the recorded imager for **grain characterization**, manual work was done with recording the minimal and maximal diameter of each particles of the given image for statistical computations. During the comparison of field and laboratory images, roughly the same volume of sediments were analysed. In most cases 1 cm^2 area of each image showed sand grains of 100 mm^3 (*e.g.* 0.1 cm^3) in total volume, what was almost equal to the acquired sample mass for one sampling attempt for laboratory analysis.

2.1 Borehole-wall imager

A **first test version** of the imager to record the borehole-wall was produced mainly to exploit the observational potential what is discussed in this work. This first version of the imager did not have the capability to move along the drilled borehole, only to record a small part of the borehole at the given depth and direction where it was let down into the hole. The imager is composed of the following units: camera house (camera, mirror, light sources), rope to move the camera and to transfer the data to a laptop. The simpli-

fied structure of the camera can be seen in Figure 1, which is an A4 Tech webcam with 640x480 pixel resolution. The illuminating source was white LED, the spectral coverage was 410-750 μm. Two types of illumination geometry were used: a grazing and a direct illumination, in order to test the consequences of different illumination angles.

Based on the experiences gained with this first test version, a **fully built second version** was realized (called hereafter borehole-wall imager, BHWI). The structure of this BHWI can be seen in Figure 2. The main components are: mount (based on a tripod) to keep the components, orient and move the camera house toward the borehole; camera house with camera and side looking mirror, illuminating LEDs; telescopic boom that accommodates two wires inside (for the camera and for the illuminating LEDs). The system was guided from a laptop and batteries were used to supply the motor. Two encoders provided feedback to the laptop on value of the realized movement, including to allow control and adjustment if necessary.

The **boom** is flexible only in sideward direction (able to easily bend perpendicular to its long axis). The **movement system** is composed of two electrical motors and two gear (wheel) systems, with one DC motor located in a fixed position to produce the vertical movement, while the horizontal movement is provided by a Pololu motor in the camera house, that rotates the camera together with the mirror below it.

The system is capable to work inside different sized boreholes, ranging from 2.5 to 4.0 cm in diameter. The camera house is a 20 mm diameter aluminium tube that accommodates the horizontal rotation motor, the camera, the mirror and the illuminating LEDs. The wheels were 3D printed from plastic and consist of two cone shaped wheels that support keeping the boom in the central position.

The camera itself is a modified version of the "USB2.0 Endoscope Camera". The CMOS 1600x1200 pixel resolution detector, records 24 bit colour images with fulfilling IP67 safety requirement. It provides the images through a 5 m long USB cable to a laptop. The data readout happens on the laptop through an USB cable with between 5-20 frame per second rate. The field of view is about 30°, the spatial resolution of the system is around 0.1 mm from 4-6 cm distance. Altogether 4 natural light LEDs were built in next the mirror to provide relatively homogeneous lighting of the borehole-wall. For directing of the movement motors and the image recording, the same software worked in a laptop, which could be used by manual activity by the operator and both by automatized (predefined) sequence of steps also.

Electrical supply for the motors and LEDs came from small batteries (<1 kg) composed of eight 1.5 V sized AA batteries or rechargeable accumulators. The spectral emissivity distribution of the used LEDs ranged from 410 to 750 nm, with producing the highest intensity around 600 nm, thus around the orange colour. The same C++ software for Windows called ImaGeo (developed for the drilled core scanning by Archigeo Ltd. and modified according to the needs) regulated the whole scanning procedure and also the image processing steps.

Image recording happens first during the horizontal rotation of the camera house. The ideal image number to covert the full 360° angular diameter section of the borehole-wall is around by 10-14 images, what could be adjusted before the start with the software. S after each horizontal imaging sequenceecondly vertical movement happens in the imaging sequence in ideal case upward to avoid the camera house got stuck (the ideal movement is roughly around 2 cm).

The **mosaic of the borehole-wall** is compiled from the small images recorded by the BHWI during the sequence according to its horizontal and vertical movement. The positions of certain images could be identified according to their filename, what is generated automatically and contains the number of row (vertical depth) as a 3 digits number first, and the number of columns (horizontal azimuth), which if properly read would make up the mosaic. The software arranges the recorded images in the form of a matrix, supported by the filenames and the ancillary data file (exact movement data with 0.1 mm and 0.1 degree accuracy).

Further adjustment of segments is supported by an artificial intelligence software that searches for similar pattern (shape and intensity changes with the given filter size) at the predefined overlapping area of the neighbouring image segments. The software called ImaGeo was developed by the ArchiGeo Ltd. marks the proposed matched point pairs, what could be accepted or rejected by the user. Manual matching could be also done, and any number of position pairs could be accepted or rejected at once. Based on the laboratory tests, the errors in the result of the mosaicking are around 1% (in terms of distances of image segment size).

2.2 Performance indicators of the BHWI

The spatial resolution of the second version of the camera was tested with grid and star shaped target objects. The resolution under ideal conditions was 52 pixel/mm, that means around 0.02 mm spatial resolution, *e.g.* 1300 dpi. The resolution changed along the field of view but was better than 0.1 mm at every location of the image. The depth of focus was tested by recording the same object form different

target distances. Higher than 0.1 mm/pixel resolution could be achieved along 4-6 mm target distance range. Geometric correction is to be done during the post processing phase. The colour calibration is to be done by recording colour code matrix containing different RGB colour code fields and compared to the original chart.

Although no substantial colour differences could be identified during the test tube scanning, certain parts of the target were brighter or darker, as an automatized correcting algorithm was implemented into the system. A small part of each recorded image covers a brightness reference palette that allows to calculate white balance with the interpretation software to correct each image according to the comparison of the same palette at different images. RGB colour codes are identified for the reference palette, and an algorithm calculates the correction to be applied on each image by the software to make them comparable.

During the tests the orientation and distance of certain recorded images were analysed. The edges of the recorded images found to be parallel aligned to each other and during the translation of the imager no distortion could be identified down to the spatial resolution.

The system works relatively fast, one full horizontal circle could be scanned ≈ 8-12 seconds + 2 second backward rotation to the starting position. The vertical movement happens in 4-6 seconds, and further 1-2 second idle time might emerge. As a consequence, for example a 10 cm long borehole-wall section could be scanned in ≈ 5-6 minutes, a 1 m segment in around half hour.

3 Results

In this section various examples are presented to demonstrate the effectivity of the system on planetary analogue materials. First rock samples in the laboratory were imaged of the first imager (to see its capability), secondly observations of field targets are presented for the first camera version, while thirdly field results of the fully built BHWI are also presented. The future usage and potential capabilities on various planetary bodies (mainly on Mars) are discussed in the Discussion section.

Figure 3 shows the testing of the general performance on Mars analogue rock samples to see specific observational characteristics of various geological features (grains, voids, layers etc.). Figure 4 shows a field of view around 9.5*5.5 mm of different rocks, which were recorded at the rock store of the Department of Petrology and Geochemistry of the Eotvos Lorand University of Sciences, Hungary.

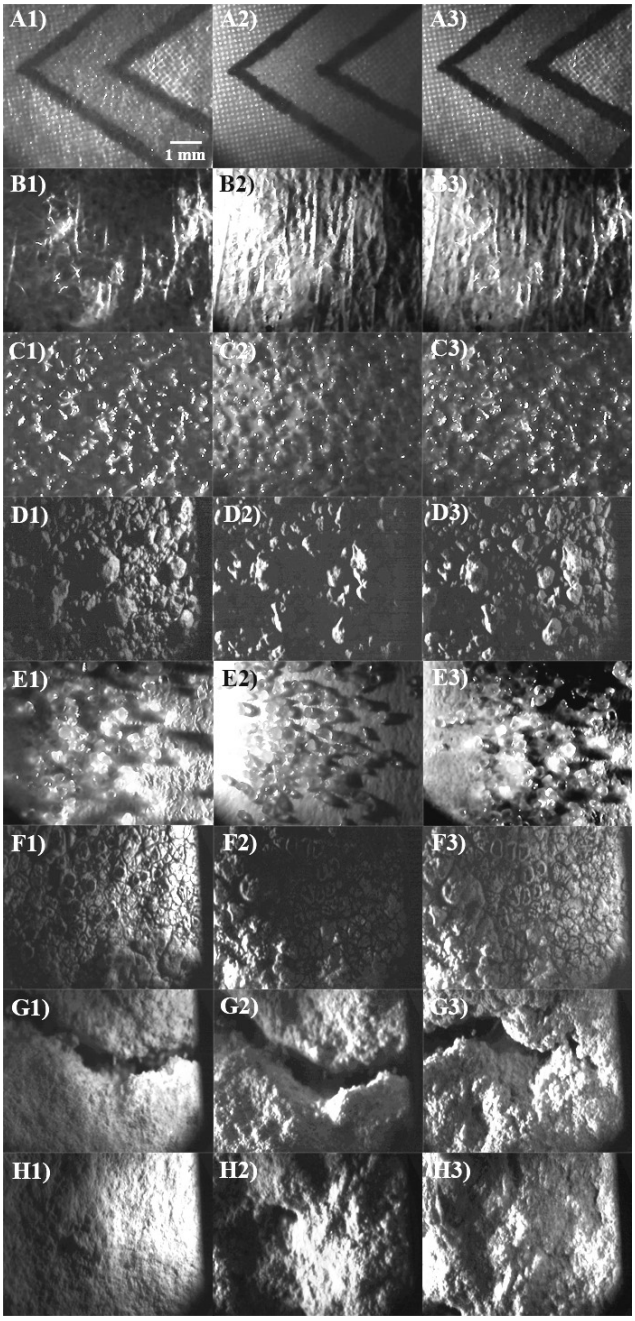

Figure 3. Results of the laboratory tests with the first camera version to see the differences between two illumination types with of grazing and direct orientations. The first column of the matrix shows the target with the grazing illumination, the second shows the same target with the direct illumination and the third column shows the same target using both illumination types. The objects of the tests (from top to bottom) are: reference colours (A1-A3), rough surface paper (B1-B3), sandpaper (C1-C3), Mars analogue sand (D1-D3), Sahara sand (E1-E3), bacterial colonies covered rock surface (F1-F3), cracks of rock (G1-G3) and sandstone surface (H1-H3).

The images in Figure 4 are arranged into pairs A and B, C and D with larger (15 cm) and smaller field of views (around 9.5*5.5 mm with double lightning) respectively, thus two samples are presented in these rows.

The specific features of the images are listed below:

1. A conglomerate is shown in A, while B picture shows specifically firmly cemented coarse gravel of mainly quartz. Grains (1-5 mm diameter) of the layer can be identified separately. 1 C,D: Depressions left behind after around 0.5 mm diameter grains fell out and as dark pits became visible at their locations.
2. The pictures (2A, B) from the siliceous limestone show layering (almost vertical layer on 2B) and scratches by the cutting process (the lines from the upper left peak to lower right peak on the 2B). Precipitation of manganese dendrite can be seen on the 2C, D pictures as little black spots.
3. The amygdules of a basalt sample are impressive on 3A and B, which are mainly elongated with different sizes.
4. The phanerocrystals (perceptible to the naked eye) from basalt lapilli and amphibolite andesite rocks are shown on the 4A and 5A and they can be identified easily (4B, 5B). However the border between the sandstone and the chert layer is not recognized on the borehole-wall images (6B), even though this border can be identifed from macroscopic pictures well. Further examples on the observable features could be seen in 7 and 8 insets.

Based on these observations, the well identifiable features in the camera photos are: separate grains, layers and border with higher contrast, depressions left behind by the fell out grains. But the separation of grains is difficult in the case of clay, aleurite and fine sand. Based on the performance testing fine scale topography as well as colour and albedo differences could be also identfied.

3.1 Field images

In the followings the results of field analysis by the simple first camera and laboratory analysis of the samples acquired in Morocco can be read. The borehole number 0601 in one of the wadi beds (at 30,984° N; -7,151° E) can be seen in the image mosaic of the borehole-wall scanned image (Figure 5). The 3 cm long vertical section at left is to demonstrate the general appearance of the various grain related features and their changes in their original environment, while at right magnified insets are to visualise some characteristic selected, small scale features of a drilled hole in the granular strata.

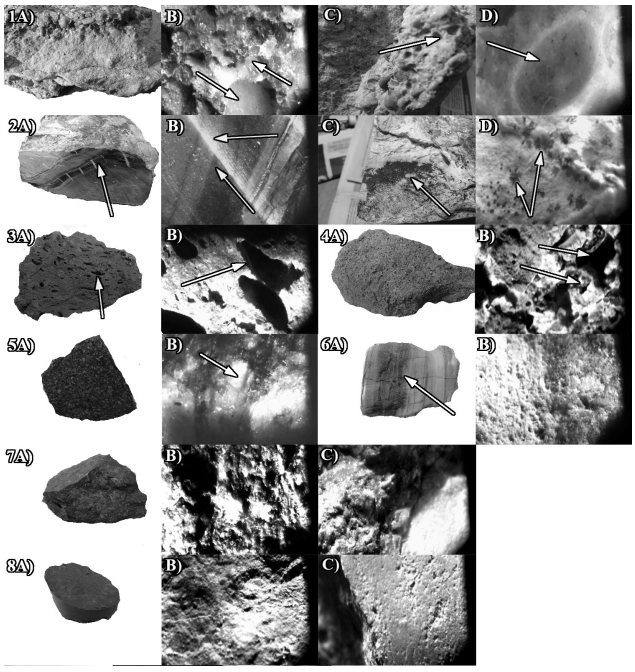

Figure 4. Images of the hand specimen of different Mars relevant type of rocks. Conglomerate and sandstone from Dunavarsány (Hungary) (1 A,B,C,D); contact metamorphic, siliceous limestone (2 A,B,C,D); amygdule basalt from Ság-hill (Hungary) (3 A,B); oxidised basalt lapilli (4 A,B); phanerocrystalline amphibolite andesite (5 A,B), chert and clay sandstone from Dunavarsány (6 A,B); hyialoclastite breccia after chloritaziation (7 A,B,C); Bodai claystone (8 A,B,C); Jakabhegyi sandstone (9 A,B,C). Interesting small scale features are indicated by arrows (see the text for more details).

The first (1) inset is a good example to demonstrate some specific aspects of scanning a borehole-wall in soft and fragile sediment with high resolution. During the drilling process, large (cm sized) blocks of the less cemented parts of the wall could fall out, leaving behind depressions. The deeper surface of such depressions is out of focus, thus appear as blurred part on images. Only some basic information could be gained at such locations like the existence of grains and their rough size. On the second inset (2) one of the bigger, clearly visible particle can be seen to demonstrate that larger grains (with diameter of 1 mm) show small scale surface features. Here the rounded edges, the roughly homogeneous surface colour and albedo can be seen. The third (3), fourth and fifth (4, 5) insets are to illustrate that smaller grains stick to bigger one, and examples for more and less rounded grains could be also seen here. The last inset (6) illustrates examples of the smaller particle range.

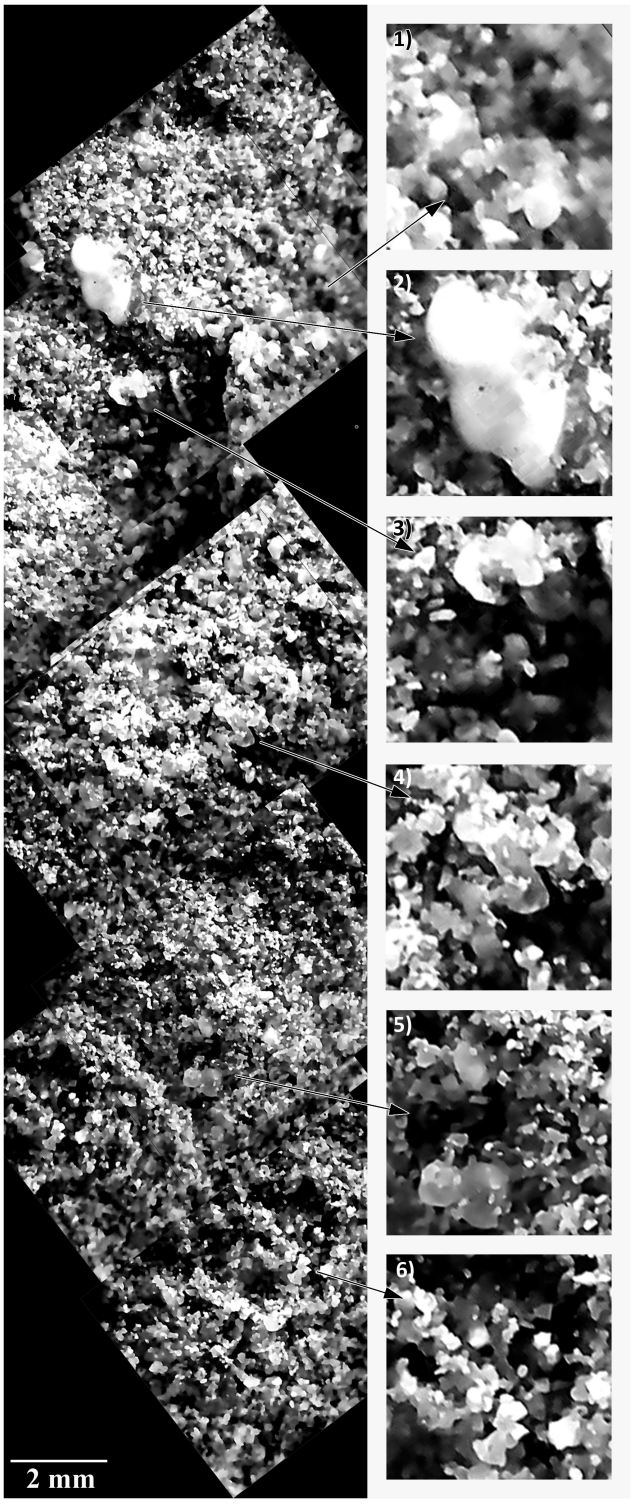

Figure 5. Section of the borehole wall can be seen on the left side, which was recorded from a drilled borehole (0601) in one of the wadi beds (30,984 N; -7,151 E) with grazing light (1*1 mm). Magnified insets on the right show interesting parts of the target, the images were recorded in the east asimuthal direction.

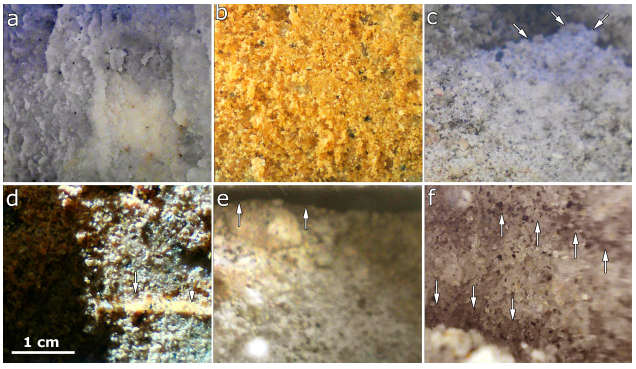

Figure 6. Example borehole-wall features from the Atacama desert.

Further examples on the borehole-wall appearance from the field tests in Atacama desert are visible in Figure 6. These images were acquired at Laguna Santa Rosa and Laguna Verde that provide examples for the following observations: a) cracked wall of a dried-up lake clay sediment, b) iron rich reddish sandstone grains, c) edge of a large aggregate (marked by arrows), d) prepared bright layer, e) dark layer at the top, f) two diffuse edge layer that could be identified only by the more frequent occurrence of darker mineral grains.

3.2 Comparison of field and laboratory tests

The overview of differences and similarities of the data on samples acquired from different depth can be seen in Table 1. It is found that along with the decreasing sorting value of the minimum particle size is relatively stable, while the maximum and average particle sizes change, increasing from the top toward down. The shape of the particles resemble in all layers: angular grains with sharp and sometimes blunt edges, while rounded and spherical particles are rare in all layers. The clay content changes along the vertical strata, it is minimal at depth 4 and 10 cm while evaporite is also present, the clay often stick to the grains in depth 30 and 40 cm. The amount of the aggregates changes within the vertical strata too. Aggregates are rare from depths of 4, 30, 40 cm, while quite frequent in the 10 cm deep layer, inside an evaporite dominated layers. The shape and the size of the aggregates range from 0.5 cm to 4-5 cm. The cementation of aggregates is usually poor/weak (they can easily go to pieces) except for this 10 cm deep layer. The identification of minerals was difficult from the field pictures, but quartz and carbonates could be present probably.

The findings from the comparison of field to laboratory observations of the same target samples are summarized in Table 2 with three observation types: borehole-wall imag-

Table 1. Analysis of the different samples from different depths of the 0601 drill from Morocco (see Figure 8). The table shows: size of the separated grains, type of minerals, morphologic features and aggregates. *Black minerals could be: magnetite, chromite, hematite, amphibolite or pyroxene.

sample depth (cm)	particle size range (average min. max.)	mineral types (by optical microscopic analysis)	particle shapes	occurrence of attached clay minerals, agglomerates
1 cm	aleurite (0.002-0.02 mm); aggregates (around 1 mm-max. 0.5 cm diam.)	quartz, carbonate minerals (calcite), mica (muscovite, biotite), Fe-oxide, black minerals*	typical shape is not visible, rounded particles are rare, angular grains with sharp and sometimes blunt edges are frequent	aggregates are poorly cemented by limonite, smaller (clay, aleurite) particles often stick to the larger grains
4 cm	aleurite (0.002-0.02) - coarse sand (0.02-2 mm) aggreagates (max 7 mm)	quartz, mica (biotite) Fe-oxide, black mineral (amphibolite) carbonate minerals, some greenish mineral	angular grains with sharp and sometimes blunt edges, rounded grains are rare	aggregates are weakly cemented
10 cm	clay (<0.002 mm) - coarse sand (0.2-2 mm) aggregates: max 1 cm	quartz, carbonate (calcite), Fe-oxide, mica (biotite), some black minerals	white precipitate on the grains, these particles are more rounded, than in the above cases	lot of aggregates, which are cemented by limonite; the bigger aggregates are strongly cemented than the smaller, single grains are well visible
30 cm	aleurite (0.002-0.02) - 5 mm (fine gravel) aggregates (2 mm-7 mm)	quartz, carbonate, Fe-oxide minerals, some biotite	angular grains with sharp and sometimes blunt edges, rounded particles are very rare	clay particles often stick to the bigger particles, aggregates are rare
40 cm	clay (<0.002 mm)- max. 2 cm (fine gravel), aggregates (few): around 0,5 cm	quartz, Fe-oxide, black minerals (difficult to identify)	the particles are usually rounded, but sometimes they have blunt edges	aggregates are poorly cemented with limonite, clay sticks to the bigger grains
evaporite layer	aleurite (0.002-0.02) - 5 mm (fine gravel), mainly aggregates (crust fragments) and separated particles	quartz, mica (biotite, muscovite), dark minerals, carbonate, evaportie	debris of rock and mineral grains: angular with sharp and sometimes blunt edges, rounded particles are rare	cement material: limonite and clay that supports aggregates
clay layer	mainly aggregates (0.5 mm-5 mm) clay (<0.002) - 1 mm (coarse sand)	quartz, carbonate, green minerals, Fe-oxide	separated particles are rare, but they are rounded, aggregates are crust fragments	aggregates, that are poorly cemented with limonite, the bigger aggregates are strongly cemented, clay contamination of grains are frequent

Table 2. Analysis of the different samples from different depth of the 0601 drill in Morocco. The table shows: size of the separated grains, type of minerals, morphologic features of the grains and the aggregates. *Black minerals could be: magnetite, chromite, hematite, amphibolite or pyroxene.

depth	borehole-wall camera field pictures		borehole-wall camera laboratory pictures		laboratory pictures with microscope	
	identified mineral types	type of minerals	identified mineral types	type of minerals	identified mineral types	type of minerals
4 cm	2	quartz, carbonate	4	quartz, carbonate, Fe-oxide, dark minerals*	6	quartz, carbonate, Fe-oxide, dark minerals, mica, clay
10 cm	1	few bright grains (carbonate?)	2	clay, dark minerals	6	quartz, carbonate, evaporite , dark minerals, clay, chlorite
30 cm	1	few bright grains (carbonate?)	4	quartz, carbonate, Fe-oxide, dark minerals	5	quartz, carbonate, dark minerals, Fe-oxide, clay
40 cm	2	quartz, carbonate	4	quartz, carbonate, clay, chlorite	4	quartz, carbonate, dark minerals, clay
evaporite layer	1	quartz	3	quartz, carbonate, clay	7	quartz, carbonate, mica, evaporite, Fe-oxide, green-, and dark minerals
clay layer	2	quartz, Fe-oxide	1	clay	5	quartz, carbonate, clay, mica, dark minerals

Table 3. The results of the particle analysis, made on the field and the laboratory pictures can be compared to in this table. These analysis were made on the pictures from the 0601 drill borehole.

depth	field pictures by borehole-wall camera						laboratory pictures by borehole-wall camera					
	min. diam. (µm)	max. diam. (µm)	average diam. (µm)	elongation	max. elong.(µm)	average diam. (µm)	min. (µm)	max. (µm)	average (µm)	elongation min. (µm)	max. (µm)	average (µm)
1 cm	67.4	587.4	204.4	0.37	0.83	0.6						
4 cm	127.2	659.9	335.6	0.31	0.98	0.69	107.4	696.3	299.3	0.44	0.99	0.76
10 cm	54.8	692.2	200.9	0.33	0.93	0.67	66.6	356.5	166.9	0.42	0.99	0.71
30 cm	95.8	580.4	322.9	0.4	0.97	0.66	95.8	580.4	322.9	0.4	0.97	0.66
40 cm	137.8	1927	502	0.4	0.99	0.7	81.8	1377.2	569.1	0.44	0.91	0.73
evaporate layer	99.9	717.8	254.1	0.46	1	0.7	56.5	407.9	175.3	0.48	0.97	0.73
clay layers	69.8	460.4	231.8	0.37	0.99	0.75	55.8	269	134.7	0.56	0.99	0.77

Table 4. Summary of numerical differences between the field and laboratory data based images using the same camera, analysing the layers of the 0601 sampling site. (X value: the longest diameter of the grains, Y value: the shortest diameter of the grains, which are perpendicular to each other).

sample depth/	4 cm		10 cm		40 cm		evaporate		day	
characteristics	field	lab	field	lab	field	lab	field	lab	field	lab
number of data points	28	39	40	48	25	20	14	54	25	34
X range (μm)	185-660	160-700	65-700	95-350	145-1930	110-1380	140-720	75-410	115-460	65-270
X average (μm)	398.1	344.5	240.9	198.1	604.6	661.1	302.6	204.5	263.6	153.2
X standard deviation	134.3	120.0	136.6	80.53	457.3	302.6	166.6	75.77	78.07	49.97
Y range (μm)	120-530	100-485	55-565	100-260	135-1490	80-750	100-425	55-265	70-320	55-250
Y average (μm)	273	254.2	160.9	135.8	399.5	477.1	205.6	146.1	200	116.3
Y standard deviation	114.3	74.6	107.9	49.6	310.2	191.9	100.7	52.3	66.6	39.2

ing, with the same camera in laboratory (under better observational conditions), and with a higher resolution regular microscope (with even better observational possibilities).

Comparing the different methods for **mineral analysis** the following findings are relevant. The least amount of information can be gained from the field pictures by the borehole-wall imager. The identification of the separate grains and the type of minerals is difficult from the field images, the most reliable estimations gave quartz or carbonate. The laboratory pictures were more informative: several types (around 8) could be identified optically, based on the colour and shape of the grains.

Those particles, which were transported by wind could be separated by their more rounded shape and sometimes bright appearance. They were found in the all layers, but were the most abundant (5%) in the evaporite and clay layers, while rare in the other layers (1-2%). Beside the mineral types, the **sizes, shapes** and related numerical values of the grains were also analysed by the same imager, comparing the observations from the borehole-wall and the laboratory samples. The results are summarized in Table 3.

Comparing the numerical information (Table 3) that could be gained from field and laboratory images with the same imager for the size and shape of grains are summarized below. The measurement of the particles' elongation was easier in the laboratory conditions than in the field, because the more difficult identification of certain grains and because their poor contrast relatively to the wall material where they were embedded. Beyond this reason, only a fraction of the particles could be identified as they were embedded in the wall – while in the laboratory, most of the grains could be analysed (except aggregates) as they were fallen apart to separated grains. Due to these factors, the estimation of the particle size or the type of minerals made in the laboratory can be closer to the reality. The comparison of numerical values acquired with the two different methods are visualized in Figure 7. It is also important to note, that all layering information were lost during the sample acquisition.

Based on the Figure 7 the distribution of data points comparing the recorded in the field and in the laboratory. The trend is similar, however small but distinct differences are also visible. Using laboratory pictures, the deviation and scattering of values are smaller along a smaller range of values. The identified maximal sized grains were bigger in field pictures in general, which can be explained with the larger field of view. But the quality of the field pictures is usually worse, so the determination of various grain related parameter is more difficult or uncertain, what causes less data.

Differences between the field and laboratory data based on Table 4 are summarized below. While the results also demonstrate that the differences between various layers **could be caught by both methods** - however the exactly measured values are different. Both the minimal, maximal and average sizes just like the standard deviation differ characteristically analysing wall images and laboratory images based measurements. The **maximal size** of the grains observed in the wall is characteristically larger than those observed in the laboratory, probably because of the general difficulty in the grain identification: larger grains were more easily identified. Beside this to have enough number of identified grains, large area of the borehole-wall should be surveyed, and the larger surveyed area increases the chance of having larger grains. The **minimal size** of measured grains were smaller in the laboratory analysis than in

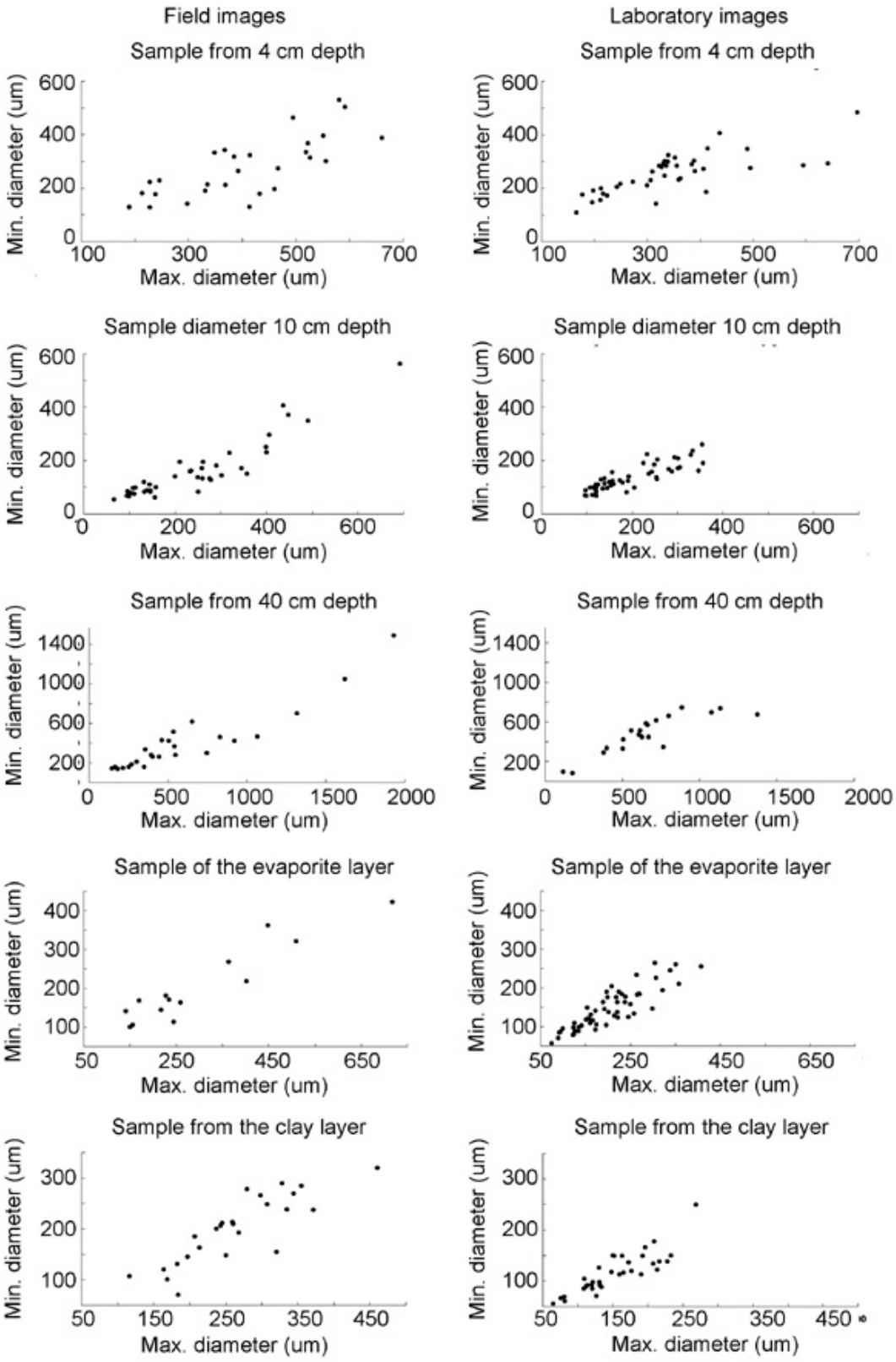

Figure 7. Diagrams of maximum/minimum diameter values of the grains from different depths based on field (left column) and laboratory (right column) pictures.

the field images, probably because of the better observing conditions there including the easier identification of separated grains than those are embedded in the borehole-wall. Both these characteristics are well known in methodology, but should be counted for the future during usage on Mars. Mainly because larger maximal sized grains identified in the field images, larger particles' size range is characteristic in the field pictures than in the laboratory pictures.

Comparing the standard deviation of the grains' diameter, characteristically different layers (for example the 40 cm deep versus the clayey layers) **differ** from each other in the deviation **between the field and laboratory images**. The reason for this is the more probable identification of **larger grains in wall images. More grains** can be identified **in laboratory pictures** despite the fact that each wall image seems to contain roughly the same number of grains (about 300-400 grains at an 5x5 mm wall area, however not all of them could be firmly identified) as in the laboratory also using 5x5 mm area. However in the laboratory separated grains rolled down from the top of each other and spread horizontally on the plate – increasing the separately visible grains' number.

Similar trend is visible in the size distribution of field and laboratory images, as points are arranged along the same trend line despite the larger scatter in the case of field images. The identification of **clay content is possible but complicated** based on the field pictures. Because of the very small grain size of clays, the identification of the individual particles is almost impossible in this small size range with the used detectors. However the clay content could be roughly estimated: as a brownish material around the bigger grains, which are strongly bounded to the surface of larger grains (Figure 6 5A, 6A) or make up aggregates (Figure 6 2A, 3A).

Comparing the general appearance of field and laboratory pictures (Figure 8) to each other, the following findings were identified. The observation and analysis of the grains were easier on the laboratory pictures: estimation of the type of minerals using only optical appearance, determination of the size and shape of the particles were more straightforward, because individual grains with their characteristic colour and shape can be seen more clearly. Certain parts of the field recorded images could be blurred and out of focus, so the contour of the grains were more difficult to the identity, making the estimation of the mineral type also uncertain. Flat crusty character of the evaporite and subsequent clay layers can be seen on the field pictures (Figure 6 5A, 6A), but this feature is rare in the laboratory pictures, because the majority of the aggregates and the fragile layer collapsed/fragmented. "Shiny" and scratched surfaces of grains can be seen well in the laboratory pictures, while the observability of these features is worse in the lower quality field images. Because of this, recognition of foreign origin grains (for example aeolian grains among fluvial ones, which are usually much more shiny as being highly polished) is almost impossible in the field pictures.

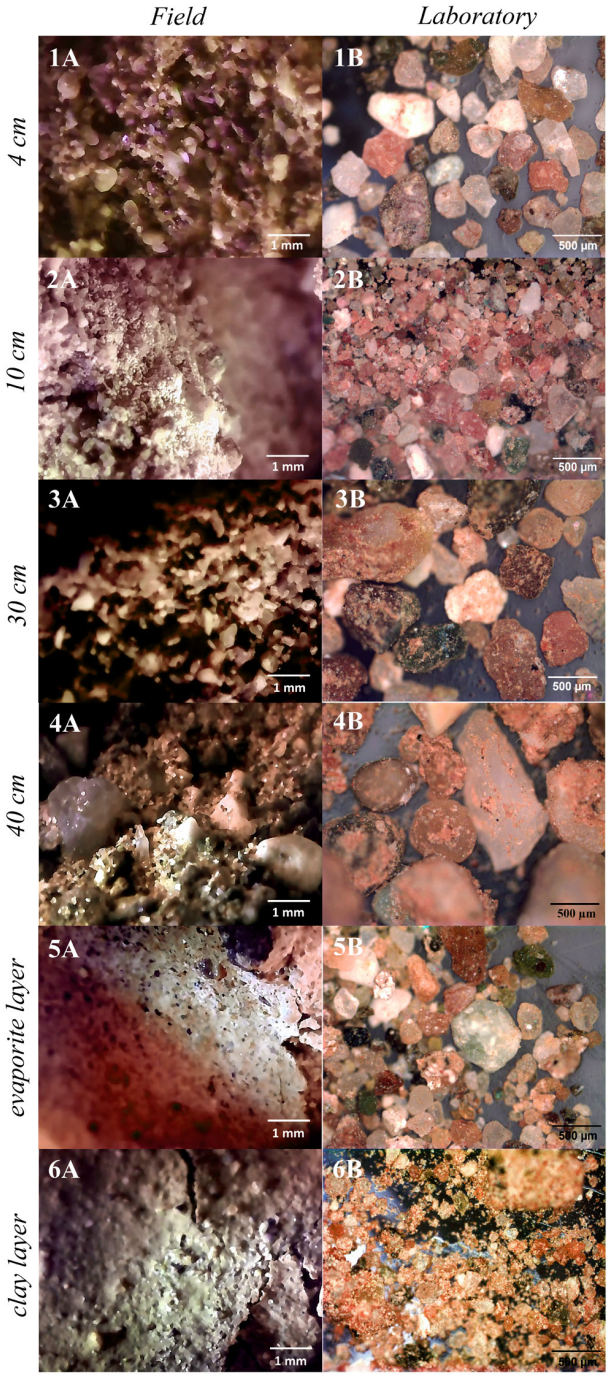

Figure 8. Images recorded by the borehole-wall camera in the field (left column) and in the laboratory (right column) from the same layer (in the same row) at the 0601 sampling site in the wadi area. Note the different scale between the left and the right columns.

Table 5. Characteristics of the deposited sediment of the different transport mode in general with the comparison aspects that could be estimated from the field and laboratory pictures.

observable characteristics	deduced formation conditions for various transport modes				estimation of characteristics using field images	estimation of characteristics using laboratory images
	wind	river	glacial ice	mass movement		
maximal grain size	coarse sand (0.5-1 mm)	gravels (>256 mm)	boulders (>256 mm, occasionally up to several m size)	boulders (>256 mm, including m - 10 m sized ones)	Can be better estimated from field pictures, because of the larger sample → supports the better identification of the high energy regime of the transport mode.	More accurate determination of the recorded grain size, however one sample is smaller than the field scanning could cover thus maximal grain size might be also smaller. As the observed range is more important → supports the more accurate transport method determination for low energy conditions.
grain size range	clay (<0.004 mm) – coarse sand (0.5-1 mm)	clay (< 0.004 mm) – boulders (>256 mm)	clay (< 0.004 mm) – boulders (>256 mm)	clay (< 0.004 mm) – boulders (>256 mm)	The identified range is shifted to larger values than the real ones because smaller grains are difficult to be identified, existence of clay size range is only indirectly suspected → weathering of the source area could be less constrained	Excluding the few largest grains, the size range could be exactly determined, thus the transport mode could be well estimated, indication on weathering state by identification of clay minerals is also possible.
grain shape	regular, rounded-well rounded	irregular: angular, subangular sometimes subrounded	very irregular: very angular-angular; but may rounded in fine range	rounded irregular, angular, subangular grains	Because of the general difficulties in grain shape estimation, the level of roundness is poorly determined, thus the separation of fresh and mature sediments, wind and water transport modes could be less accurate.	The better information on the shape of the grains supports the identification of transport mode, and with the maturity of the deposit supports to estimate the scale of active duration of the transport process.
mineral type	monomict (mainly quartz)	oligo-, poligomict	oiligo-, poligomict	oligo-, poligomict	Few type of minerals can be identified → poorly known compositional characteristics of the source regions.	Much more minerals can be determined, even various levels of in between different maturity of sediments transported by similar method could be estimated/separated.
clay mineral fraction	minimum quantity	significant quantity	present	present	The presence and amount of clay fraction could be estimated only indirectly → weathering state of the source region could be poorly constrained.	The amount of clay fraction can be better determined, what supports to estimate the level of earlier interaction with water for different sediments.
layering	graded bedding or cross-stratification	parallel laminated → calm or very fast flow condition graded bedding or cross-stratification → fast condition	unstratified	unstratified, chaotic layers, sedimentary fold, grading or inverse grading in layers → determination of mass movement type	Layering could be identified, including the size and sequence of layers → pointing to the temporal changes in the depositional conditions.	Layering cannot be seen in the laboratory pictures → related aspects of the depositional process remain unresolved.
imbrication	-	ordered fabric → flow direction	-	ordered fabric → flow direction	Imbrication can be identified → might point to flow direction and support the determination of transport mode.	Imbrication cannot be seen in laboratory pictures, all related information is lost.

Table 6. Characteristics of the typical sedimentary structures: material type, size of the layers and the fact could they be observed in the field pictures from the borehole. The "ideal situation" means the identification is possible however the conditions that allow (size an configuration of grains, colour and albedo differences, size and direction of shadows from illumination that support the data acquisition etc.) it are probably rare.

observed characteristics of sediment	material type	size/ thickness of the layers	is it easily observed in the borehole in field pictures ?
silt/clay sheet	clay/silt (on the sand layer)	mm - max. 1-2 cm	yes
clay flaser	clay (on the sand layer)	mm - max. 1-2 cm	yes
planar stratification in clay	clay	depends on the thickness of the layer (average 3-4 cm)	yes
tabular cross bedding	sand	thickness of sets >5 cm [53]	yes (only part of it, but some conclusion can be suspected)
ripple cross bedding	sand	thickness of sets >5 cm [53]	yes (only part of it, but some conclusion can be suspected)
wedge shaped cross bedding	sand	thickness of sets >5 cm [53]	yes (only part of it, but some conclusion can be suspected)
planar stratification in sand	sand	thickness of sets <5 cm [53]	yes
flame-, ball or pillow structure (from water escape)	mainly sand	from a few cm, to around 10-15 cm	only in ideal situation
polygonal structures (from drying)	clay, sand, gravel sized blocks	few cm to several meters [52]	only in ideal situation

Some **methodological experiences** were also gained during the field and laboratory work: High resolution of borehole-wall imaging is difficult to acquire partly as the borehole-wall need not be perfect cylinder shaped. In the case of inhomogeneous vertical cementation and elevated mechanical strength of the strata, certain layers might become more fractured by the drilling process. Here more material falls out of the wall, and the wall there might be larger distance from the camera, thus out of focus. Specific findings could be more easily identified as vertical changes. Combination of grazing and direct illumination provides the most information about the sediment (both on structures, boundary of layers, stratification, and also indicators of surface texture and colour).

4 Discussion

Based on the comparison of the field and the laboratory recorded images, different observations could be realized that provide different possibilities for the estimation of the characteristics and the origin of the given sediment. Below we discuss first what type of observations could be realized more easily with one of the two methods and which is the ideal for a given task. After this a methodological summary can be read and finally the overview of the relevant aspects of the Mars mission are presented.

Measuring the sizes of grains, differences are identified between images recorded in the field and in the laboratory: more grains and larger particles' size range can be identified in the laboratory pictures mainly because of the smaller identified grains with this method based on the better quality images. In the field images larger grains could be identified more often, but large part of a given grain is poorly visible in the field pictures. These selection effects are caused by that field images were recorded under less ideal conditions, and that the observability of a given grain might also differ if it is embedded in the wall or pulverized as separate grains, even if the observing conditions are the same.

These observational effects influence the interpretation in the following ways:

- The decreased accuracy of **size distribution** measurements in the field causes larger deviation from the average relatively to laboratory pictures. The minimum diameter is 29-40% and the maximum diameter is 33-46% **in the case of the laboratory pictures than in field images**, meanwhile the minimum diameter changes 33-77% and maximum diameter changes between 30-55% **in the case of the field pictures**. The laboratory pictures provide more accurate information about the maximum and minimum particle size thus level or **sorting of grains**.
- Based on the measured size differences between the laboratory and field pictures, the **classification of the grains** is shifted toward the larger fraction size using field data, suggesting a bit more energetic transport and/or depositional conditions.

- The **shape** and the circularity of the grains is difficult to determine in the field pictures, because the whole grain can not be seen or its outline is hardly identified. However if the grains have strong colour contrasts relatively to the environment or the matrix, they could be analysed precisely. Because of the less information on the roundness and surface pattern of the grains using field recorded data, the selection of transport agent is more difficult, as well as the type of origin, thus the identification of water related potential habitability of the environment.
- **Less grains** could be identified from roughly the same volume of target material in the field. Twice or three times as many minerals were identified from the laboratory than from the field pictures, mainly because of better image quality and smaller observable details (of colour and shape), and only partly because more grains can be seen in laboratory pictures.
- The **clay content** of the sediment could be identified more difficulty from field data not only because of the small size of these grains, but also because they stick together and form aggregates. However the presence of these small grains could be suspected as they appear as cement or surface covering material in the field pictures. The clay content refers to the presence of less resistant minerals and wet weathering of the grains before or during the transport.
- The laboratory pictures are more informative for the **shape, and surface pattern** of the grains and origin of the sediments (the transport medium and maturity can be estimated from the smoothness and circularity of the grains, the sorting of sediment can be connected to the energy of the medium), while field images provide information on the depositional conditions based on layerng.

Methodological experiences with the imager provided the following results: grazing and direct illuminations are useful for different types of analysis. While for surface roughness analysis grazing light is better (supporting grain identification, shape determination, identification of the structure of layers, identification of weathering/falling out of the individual grains), colour and albedo differences could be seen better with direct light (for mineral type estimation). However based on the experiences using of direct and grazing illuminations, they provide the best results together. **Identification of individual particles** is difficult in the field pictures, because of the embedded location of the particles in the wall only a smaller fraction of each grain is invisible. This problem may influence the determination of the true particle size and thus of the sorting of the sediment.

4.1 Extrapolation to Mars

During future Mars missions, in-situ recorded images might get more importance as the target should be better characterized in real time and used for the selection of ideal ones, especially during the selection in the case of samples for Mars sample return (Sephton et al. 2013). This will increase the efficiency of the work, thus a fist on-site imaging survey supports to estimate such characteristics of a sample (grain size, rough size distribution) that only a moderately detailed on-site laboratory work will provide. Small sized fluvial and lacustrine grains composed deposit have elevated potential for organic material preservation (Westall et al. 2009), thus in astrobiology aimed research project might be easily targeted. Summary of Mars relevant aspects focusing on the analysis of sedimentary origin on the material can be read in the Table 7.

During the drill in case of optical images recorded like those presented before will definitely help to identify the best location to sample for return or more detailed in-situ analysis. For the separation of eaolian, fluvial, ice or mass movement related sediments, the spatial resolution (around 0.1 mm) is enough based on analogue examples tested on the Earth.

The accuracy to determine the size of grains and **sorting of sediments** differ for the minimal and maximal sizes: the smaller particle size range (clay–aleurite grains) can be identified better in laboratory pictures while the extremely large grains are easier to find in field recorded images, what cause an overestimation of mean grain size using only field relatively to laboratory images. The type and speed of the transport medium estimated from the sorting of the sediment (like fast or slow river) could be also influenced and shifted to preferred larger energies using field images. The possibility that larger number of **mineral types** should be determined in laboratory makes easier to estimate the source region and the order of transport time. The **shape and morphology of the grains** (roundness, circularity, angularity), can be better determined from the **laboratory pictures**. The shape of the grains helps to determine the transport medium, while the clay content depends on the weathering potential (the larger is the amount of clay, the more warmer and wetter might be the conditions supporting the weathering process) – this directly helps paleoenvironmental reconstruction.

Using borehole-wall scans the **determination of layering** (parallel, cross laminate/stratification, type of cross

stratification, etc.), the sequence of these layers above each other, the **grain orientation** (imbrication), just like the **grading and deformational structures** can be seen in the **field pictures** – while such information is lost during the sample acquisition and cannot be determined from laboratory analysis. This fact points to that for the estimation of depositional conditions (for example water or ice or wind transport method, existence of waveing bulk or drying up less liquid water during deposition) could be much better estimated from field images than laboratory data. However clay and bound water content could be determined from the acquired samples too, also pointing to wet weathering in general.

Table 6 gives a summary of these potential sedimentary features that help in the estimation of the transport mode. Some examples to demonstrate that borehole-wall based data provides information on the paleo-environment, (while such information could not be gained from acquired sample) are listed below:

- Standing condition (river, reef) of medium: siltsheet, clay flaser (where the underlying sand is covered by mud layer of only some mm, that point to sedimentation from water rich period and several even separated wet periods might be conserved;
- planar stratification in clay: quiet flow or very slow transport system;
- tabular cross bedding, through cross bedding, wedge shaped cross bedding, which might point to winds and various density currents, exact determination of the transport medium requires the joint analysis of sedimentary features and the characteristic grain size;
- ripple cross bedding, planar stratification in sand support the estimation of flow direction and speed of the flow (Froude number >= 1 (Tucker 1995));
- drying polygons, mark of rain drops point to the ephemeral existence of wet conditions (W. S. 2009; Tucker 1995);
- the upward direction of the sediments could be determined only from borehole-wall scanning, that helps to estimate some further parameters during sediment deposition (like density difference between two layers, rapid sedimentation, when before the consolidation of the already deposited sediment a new layer starts to settle down and their temporal changes).

A general problem on Mars is the poor knowledge about whether the clay minerals were transported to a given location from another site or were they formed in-situ there. The determination of formation site of phyllosilicates supports the understanding where were the conditions favourable for the emergence of liquid water or even life. To achieve this knowledge, the coupling of borehole-wall images (pointing to the possible existence of wet signatures with depositional features etc.) and laboratory based OH containing chemical and mineral data (pointing to past wet weathering) is helpful together.

Without the borehole-wall analysis the sequence of the events and the condition of sedimentation cannot be determined well. Transport medium, mode of the transport and of deposition (transport time, speed and sedimentation hiatus) could be characterized more accurately if the field and laboratory imaging methods are used together. At the same time several other parameters (number of mineral types, shape and morphology) are better constrained from laboratory data.

The borehole-wall based sedimentary analysis on Mars might be better realized and provide more information on Mars than on Earth especially for old sediments. Because of plate tectonism, related burial, elevated geothermal gradient and metamorphism on the Earth, old sediments have poor retention regarding of features that point to their original formation conditions. Opposite to this, the situation is different on Mars, because of the lack of global plate tectonism and the small geothermal gradient, even the oldest sediments might easily hold sensitive indicators for the ancient conditions (layering, gradation, imbrication etc.). Beyond this while on Earth boreholes are usually filled with water or mud, on Mars they are expected to be empty, providing good visibility of the wall. During a drill produced sample acquisition, substantial part of the above listed information will be lost except if borehole-wall scanning will be done – thus it helps to identify the ideal sampling location for more detailed analysis, including biology relevant information.

4.2 Contribution in future missions

Below, we extrapolate to near future Mars mission types (Table 7) to evaluate, how much the above listed field and laboratory observing possibilities are complementary and how this knowledge might influence the planning of the given mission. As laboratory analysis is already planned, we put emphasis on what kind of further inputs could the borehole-wall analysis provide for the mission.

It is worth mentioning that the necessary imaging instruments to scan the borehole-wall are quite low cost and could be accommodated in a small volume (order of some cubic cm), and their mass and energy consumption is very low relatively to other instruments on a Mars surface mission. Thus the usage of such facility is highly preferred and

Table 7. Summary of potential contribution of borehole-wall imaging in next Mars missions. The * marks the ExoMars 2020 mission, where no optical but only infrared borehole-wall scanning is planned, thus its potential findings are listed here, while for the other candidate mission types the optical version was considered.

mission name or type	expected/ possible findings from borehole-wall observations	synergy with laboratory measurements and mission relevant aspects
ExoMars rover*	grain composition, certain level of layering	identification of rough characteristics of the source layer at the original location of the acquired sample
Mars sample return	selection of ideal target layers, sedimentary properties of layers, improved targeting to select sample to return	identification of rough characteristics of the source layer at the original location of the acquired sample possibility to correlate the drilled strata with nearby open air outcrops improved estimation of depositional conditions
crewed Mars surface mission	selection of ideal target layers, sedimentary properties of layers, improved targeting to select sample for detailed on-site laboratory analysis, specific targeting related to specific on site laboratory work	identification of rough characteristics of the source layer at the original location of the acquired sample, possibility to correlate the drilled strata with nearby open air outcrops, improved targeting of the best layer of a strata from already acquired sampled column, selection among layers regarding the capacity to trap and hold organic molecules.

further tests to develop and adapt the capability to Martian conditions are strongly recommended.

5 Conclusion

In this work some specific aspects of **in-situ field and later laboratory acquired imaging** of drilled targets at Mars analogue sites were analysed and compared. Drilling will be an important method for future work on Mars as radiation and surface chemistry destroy certain molecules and minerals on the surface. To reconstruct early wet conditions, old and buried sediments will be targeted there in the subsurface. Next missions, especially sample return and later human missions need to better understand the formation conditions and astrobiology potential of the target during the missions themselves to improve targeting to get the most relevant samples. This should be supported by on-site targeting based on the survey of the drilled borehole there. While the context (sedimentary conditions, embedding geometry, surrounding material) of the acquired sample is lost after it has been acquired, borehole-wall scanning could get this information, increase the targeting accuracy during the sampling process and also provide such information what could not be gained from the acquired sample alone.

Two field facilities were used and tested in Morocco and at the Atacama desert to identify the main parameters of borehole-wall scanning, and define what kind of characteristics of the target could be determined by this method. A fluvial wadi sediment at a Mars analogue site was surveyed and sampled at the Ibn Battuta Centre in Morocco with a specific imager to screen the drilled borehole-wall to outline the general advantages, disadvantages and complementarity of the methods. In Atacama desert, salty lakebed with clayey sediment and other desiccated locations were analysed. The recorded images demonstrated that using a simple facility spatial resolution of 0.1 mm could be achieved, and sedimentary features and various grain scale characteristics could be observed. Comparing the scanned in-situ images and the analysis of the acquired sample in laboratory, the following findings were achieved. A range of differences were identified between the field and laboratory recorded images what could influence the observability, even using the same facilities, the appearance of target depends strongly on the fact if it is embedded in its original environment or not.

Benefits of borehole-wall imaging relatively to laboratory imaging are: maximal size of grains (thus the maximal energy of the transport process) could be more easily identified (what might be important on Mars where ephemeral events including the sudden release of large water volumes might occur); occurrence of sedimentary structures (layering and their sequence, grading, grain orientation, water escape structure etc.) could be identified to understand the depositional conditions and temporal hiatus of sedimentation (*e.g.* temporal changes of wet conditions) - while these information types are almost absent in the laboratory data, as have been lost during sample acquisition. Field images showing fine powder attached on larger grains often point to clay content what is a strong environmental indicator, indicating such deposit that might have witnessed wet weathering process, what is highly im-

portant in the analysis of potential habitability of the given environment.

Benefits of laboratory imaging are the better identification of shapes and grain surface characteristics (pointing to the maturity of grains and partly the transport mode), sorting of sediments (*e.g.* the efficiency of separating a given grain size and elongation), the firm identification for smaller grain size including clay content what is important for weathering process – however indication of clay content could be already realized from field images. Although both imaging methods could provide information on the transport mode, but borehole-wall scanning tends to suggest more energetic transport conditions – however larger and more representative sampling for laboratory analysis could eliminate this difference.

Based on the above listed findings **improvement of specific field facilities** for drilling and sampling on Mars should put emphasis on the optical imaging during the drilling with targeting the wall. The recorded context together with the laboratory results of the acquired sample help to separate different water flow regimes and standing or flowing water deposits, temporal characteristics of the ancient wet condition and later changes of the already deposited material. Because of the general weak alterations on Mars, the lack of plate tectonism and small geothermal gradient, ancient sediments are not reworked there thus hold such sedimentary/morphological information on their origin, what is usually lost on the Earth but could be gained by borehole-wall scanning. As a summary the temporal characteristics and properties of local sedimentation could be better understood with screening the borehole-wall.

Acknowledgment: The field site access was supported by the Trans National Access project of the Europlanet 2020 RI (H2020 fund No 654208) and COST 1308 project, while the related laboratory work was supported by the COOP-NN-116927 by NKFIH. Based on the lessons learned the next project in joint activity with ESA was initiated to develop an advanced version of the imager to support the ExoMars mission's Earth based analogue activities. This activity was supported by the EXODRILTECH (No. 4000119270) project regarding mainly the technological development. The work was also supported by the Excellence of Strategic R&D centres (GINOP-2.3.2-15-2016-00003) of NKFIH, funded by EU R&D project.

References

Benner, S. A., Devine, K. G., Matveeva, L. N., and Powell, D. H.: 2000, *Proceedings of the National Academy of Science* **97**, 2425

Castagna, M. and Bellin, A.: 2009, *Water Resources Research* **45(4)**, n/a, W04410

Cheng, C. H.: 1981, *Geophysics* **46**, 1042

Christner, B. C., Mikucki, J. A., Foreman, C. M., Denson, J., and Priscu, J. C.: 2005, *Icarus* **174**, 572

Daily, W., Ramirez, A., Labrecque, D., and Nitao, J.: 1992, *Water Resources Research* **28**, 1429

Dartnell, L. R. and Patel, M. R.: 2014, *International Journal of Astrobiology* **13(2)**, 112-123

De Angelis, S., De Sanctis, M. C., Ammannito, E., Carli, C., Di Iorio, T., and Altieri, F.: 2014, *Planetary and Space Science* 101

Finzi, A. E., Lavagna, M., and Rocchitelli, G.: 2004, *Planetary Space Science* **52**, 83

Foing, B. H., Stoker, C., Zavaleta, J., Ehrenfreund, P., Thiel, C., Sarrazin, P., Blake, D., Page, J., Pletser, V., Hendrikse, J., Direito, S., Kotler, J. M., Martins, Z., Orzechowska, G., Gross, C., Wendt, L., Clarke, J., Borst, A. M., Peters, S. T. M., Wilhelm, M.-B., Davies, G. R., and Davies: 2011a, *International Journal of Astrobiology* **10**, 141

Foing, B. H., Stoker, C., Zavaleta, J., Ehrenfreund, P., Thiel, C., Sarrazin, P., Blake, D., Page, J., Pletser, V., Hendrikse, J., Direito, S., Kotler, J. M., Martins, Z., Orzechowska, G., Gross, C., Wendt, L., Clarke, J., Borst, A. M., Peters, S. T. M., Wilhelm, M.-B., Davies, G. R., and Davies: 2011b, *International Journal of Astrobiology* **10**, 141

Glass, B., Cannon, H., Branson, M., Hanagud, S., and Paulsen, G.: 2008, *Astrobiology* **8**, 653

Glass, B., Cannon, H., Hanagud, S., Lee, P., and Paulsen, G.: 2006, in S. Mackwell and E. Stansbery (eds.), *37th Annual Lunar and Planetary Science Conference*, Vol. 37 of *Lunar and Planetary Science Conference*

Glass, B., McKay, C., Stoker, C., Zacny, K., and Hoftun, C.: 2012, in *Concepts and Approaches for Mars Exploration*, Vol. 1679 of *LPI Contributions*, p. 4185

Gouache, T. P., Gao, Y., Coste, P., and Gourinat, Y.: 2011, *Planetary Space Science* **59**, 1529

Groemer, G., Gruber, V., Bishop, S., Peham, D., Wolf, L., and Högl, B.: 2010, *Acta Astronautica* **66**, 780

Groemer, G., Soucek, A., Frischauf, N., Stumptner, W., Ragonig, C., Sams, S., Bartenstein, T., Häuplik-Meusburger, S., Petrova, P., Evetts, S., and Sivenesan, C.: 2014, *Astrobiology* **14**, 360

Hill, J. L., Shenhar, J., and Lombardo, M.: 2003, *Advances in Space Research* **31**, 2421

Hoftun, C., Lee, P., Johansen, B. W., Glass, B. J., McKay, C. P., Schutt, J. W., and Zacny, K.: 2013, in *Lunar and Planetary Science Conference*, Vol. 44 of *Lunar and Planetary Science Conference*, p. 2817

Juck, D., Whissell, G., Steven, B., Pollard, W., P McKay, C., Greer, C., and Whyte, L.: 2005, **71**, 1035

Kapui, Z., Kereszturi, A., Ori, G. G., Taj-Eddine, K., and Ujvari, G.: 2017, in *Lunar and Planetary Science Conference*, Vol. 48 of *Lunar and Planetary Science Conference*, p. 1428

Lee, R., Sathiyanathan, K., Navarathinam, N., and Quine, B.: 2009, *Canadian Aeronautics and Space Journal* **55**, 79

Losiak, A., Orgel, C., Moser, L., MacArthur, J., Gołębiowska, I., Wittek, S., Boyd, A., Achorner, I., Rampey, M., Bartenstein, T., Jones, N., Luger, U., Sans, A., and Hettrich, S.: 2013, in *EGU General Assembly Conference Abstracts*, Vol. 15 of *EGU General Assembly Conference Abstracts*, pp EGU2013–11556

Magnani, P. G., Re, E., Ylikorpi, T., Cherubini, G., and Olivieri, A.: 2004, *Planetary Space Science* **52**, 79

McKay, C. P., Hecht, M. H., Stoker, C., Briggs, G., Clark, B., Cooper, G. A., Glass, B., Gulick, V., Lambert, J., Zacny, K., Nakagawa, R., and Chadbourne, P.: 2007, in *Lunar and Planetary Science Conference*, Vol. 38 of *Lunar and Planetary Science Conference*, p. 1468

Moores, J. E. and Schuerger, A. C.: 2012, *Journal of Geophysical Research (Planets)* **117**, E08008

Navarathinam, N., Lee, R., Borschiov, K., and Quine, B.: 2011, *Acta Astronautica* **68**, 1234

Orgel, C., Achorner, I., Losiak, A., Gołębiowska, I., Rampey, M., and Groemer, G.: 2013a, *European Planetary Science Congress* **8**, EPSC2013

Orgel, C., Battler, M., Foing, B. H., Van't Woud, H., Maiwald, V., Cross, M., and Ono, A.: 2013b, *European Planetary Science Congress* **8**, EPSC2013

Ori, G. G., Marinangeli, L., and Komatsu, G.: 2000, *Planetary Space Science* **48**, 1027

Parro, V., Fernández-Calvo, P., Rodríguez Manfredi, J. A., Moreno-Paz, M., Rivas, L. A., García-Villadangos, M., Bonaccorsi, R., González-Pastor, J. E., Prieto-Ballesteros, O., Schuerger, A. C., Davidson, M., Gómez-Elvira, J., and Stoker, C. R.: 2008, *Astrobiology* **8**, 987

Philippe, G., Tim, B., Pezard, P., and Yeh, E.-C.: 2007, *Scientific Drilling* 5

Pitcher, C. and Gao, Y.: 2015, *Advances in Space Research* **56**, 1765

Poch, O., Kaci, S., Stalport, F., Szopa, C., and Coll, P.: 2014, *Icarus* **242**, 50

Prieto-Ballesteros, O., Martínez-Frías, J., Schutt, J., Sutter, B., Heldmann, J. L., Bell Johnson, M. S., Battler, M., Cannon, H., Gómez-Elvira, J., and Stoker, C. R.: 2008, *Astrobiology* **8**, 1013

Rehfeldt, K. R., Boggs, J. M., and Gelhar, L. W.: 1992, *Water Resources Research* **28**, 3309

Sephton, M. A., Court, R. W., Lewis, J. M., Wright, M. C., and Gordon, P. R.: 2013, *Planetary Space Science* **78**, 45

Stalport, F., Coll, P., Szopa, C., Cottin, H., and Raulin, F.: 2009, *Astrobiology* **9**, 543

Stoker, C. R., Cannon, H. N., Dunagan, S. E., Lemke, L. G., Glass, B. J., Miller, D., Gomez-Elvira, J., Davis, K., Zavaleta, J., Winterholler, A., Roman, M., Rodriguez-Manfredi, J. A., Bonaccorsi, R., Bell, M. S., Brown, A., Battler, M., Chen, B., Cooper, G., Davidson, M., Fernández-Remolar, D., Gonzales-Pastor, E., Heldmann, J. L., Martínez-Frías, J., Parro, V., Prieto-Ballesteros, O., Sutter, B., Schuerger, A. C., Schutt, J., and Rull, F.: 2008, *Astrobiology* **8(5)**, 921, PMID: 19032053

Szwarc, T., Aggarwal, A., Hubbard, S., Cantwell, B., and Zacny, K.: 2012, *Planetary Space Science* **73**, 214

Tucker, M.: 1995, *Earth Science Reviews* **39**, 117

W. S., B.: 2009, *Geological Magazine* **125**, 664

Wang, K.: 1992, *Journal of Geophysics Research* **97**, 2095

Weiss, P., Yung, K. L., Ng, T. C., Kömle, N., Kargl, G., and Kaufmann, E.: 2008, *Planetary Space Science* **56**, 1280

Westall, F., Foucher, F., Bost, N., Bertrand, M., Loizeau, D., Vago, J. L., Kminek, G., Gaboyer, F., Campbell, K. A., Bréhéret, J.-G., Gautret, P., and Cockell, C. S.: 2015, *Astrobiology* **15**, 998

Westall, F., Foucher, F., and Cavalazzi, B.: 2009, in D. N. Arabelos and C. C. Tscherning (eds.), *EGU General Assembly Conference Abstracts*, Vol. 11 of *EGU General Assembly Conference Abstracts*, p. 4899

Williams, J. H. and Johnson, C. D.: 2004, *Journal of Applied Geophysics* **55**, 151

Zacny, K., Paulsen, G., Chu, P., Mellerowicz, B., Yaggi, B., Kleinhenz, J., and Smith, J.: 2015, in *Lunar and Planetary Science Conference*, Vol. 46 of *Lunar and Planetary Science Conference*, p. 1614

Zacny, K., Paulsen, G., Craft, J., Maksymuk, M., Santoro, C., and Wilson, J.: 2009, *AGU Fall Meeting Abstracts* pp P43A–1423

Zacny, K., Paulsen, G., McKay, C. P., Glass, B., Davé, A., Davila, A. F., Marinova, M., Mellerowicz, B., Heldmann, J., Stoker, C., Cabrol, N., Hedlund, M., and Craft, J.: 2013a, *Astrobiology* **13**, 1166

Zacny, K., Paulsen, G., McKay, C. P., Glass, B., Davé, A., Davila, A. F., Marinova, M., Mellerowicz, B., Heldmann, J., Stoker, C., Cabrol, N., Hedlund, M., and Craft, J.: 2013b, *Astrobiology* **13**, 1166

Zacny, K., Paulsen, G., McKay, C. P., Glass, B., Davé, A., Davila, A. F., Marinova, M., Mellerowicz, B., Heldmann, J., Stoker, C., Cabrol, N., Hedlund, M., and Craft, J.: 2013c, *Astrobiology* **13**, 1166

Zacny, K. A., Quayle, M. C., and Cooper, G. A.: 2004, *Journal of Geophysical Research (Planets)* **109**, E07S16

Zent, A. P. and McKay, C. P.: 1993, in R. Burns and A. Banin (eds.), *Chemical Weathering on Mars*